AIAA JOURNAL
Vol. 41, No. 2, February 2003

Dynamic Equivalence Conditions for Controlled Robotic Manipulators

M. Ghanekar*
Honeywell Engines, Systems, and Services, Mississauga, Ontario L5L 3S6, Canada
and
D. W. L. Wang† and G. R. Heppler‡
University of Waterloo, Waterloo, Ontario N2L 3G1, Canada

The nondimensional groups that define the dynamic equivalence conditions for general rigid-link and flexible-link manipulators are examined. The scaling conditions for friction effects and the tolerances on the nondimensional group values are also investigated. A nonlinear compensation technique is presented to allow for parameter value uncertainties. Scaling laws for general control strategies are also presented. Simulation results are presented.

I. Introduction

TO design and test robots destined for use on other planets efficiently, it can be advantageous to build, smaller, less costly scale-model prototypes. When building dynamically equivalent scale models, the dynamic properties of the manipulator, including gravity and flexibility effects, should also be scaled because, by incorporating gravity effects into the scale model, extra gravity compensation schemes will not be required when using the prototype.

Ghanekar et al.[1] used dimensional analysis to determine the scaling conditions for single flexible link manipulators and presented scaling laws for continuous-time and discrete-time controllers. Hollerbach[2] identified a time scaling property for single link manipulator dynamics that allows planned manipulator trajectories to be analyzed and modified if they are unrealizable. Youcef-Toumi and Gutz[3] used dimensionless groups to characterize impact phenomena. Goldfarb[4] studied scaled bilateral telemanipulation and Stocco et al.[5] presented a joint and task space scaling matrix for use in optimal robot design. Similitude conditions for general rigid-link manipulators[6] and for general flexible-link manipulators[7] have been presented, and Ghanekar[8] has subsequently shown the equivalence of the rigid-link and flexible-link nondimensional groups.

All physical quantities can be characterized using the seven fundamental dimensions.[9] For example, the dimensions of a force variable are expressed by $F \equiv [M][L][T]^{-2}$, where the notation $\equiv$ is used to indicate that the dimensions of a quantity are being given. The Buckingham pi theorem (see Ref. 10) provides a systematic means of determining the nondimensional pi groups that characterize the dynamics and provides scaling information for the system.

In this paper, the Buckingham pi method is used to determine the nondimensional groups characterizing rigid-link and flexible-link manipulators, and it is extended to general nonlinear controllers. The pi groups characterizing the manipulator dynamics of system 1 are computed and are then used to design a dynamically equivalent system 2. A control scheme is designed for system 2. The controller pi groups are calculated and are then used to determine the controller, which will provide dynamically equivalent performance, for system 1. Because of manufacturing imprecision it is, in practice, impossible to construct two systems that are exactly dynamically equivalent. To address this problem, a nonlinear compensation technique is presented that allows for errors in the scaling conditions to be tolerated. The scaling of friction effects is an ideal candidate for this compensation scheme, and the results of a simulation are presented.

Received 23 September 2000; revision received 20 August 2002; accepted for publication 20 August 2002.

*Senior Staff Engineer, Systems Engineering Department, 3333 Unity Drive.
†Professor, Electrical and Computer Engineering.
‡Professor, Systems Design Engineering. Senior Member AIAA.

II. Equivalence Conditions: Rigid-Link Manipulators

The phrase general rigid-link manipulator will refer to the class of manipulators with n rigid links, p actuators, and any link topology that can be described by a set of generalized coordinates that make the explicit use of constraint equations unnecessary.

To apply dimensional analysis, a complete set of variables characterizing the system dynamics must be identified. The dynamic behavior depends on the link parameters, the joint parameters, gravity, and time. The ith link is characterized by its mass $m_i \equiv [M]$, and the mass moments of inertia about each of its three principle axes, J_i^{xx}, J_i^{yy}, and J_i^{zz} ($\equiv [M][L]^2$). The jth joint is assumed to have mass $M_j \equiv [M]$ and rotational inertia $I_j^h \equiv [M][L]^2$ about the joint axis (rotary actuators only). Acceleration due to gravity is denoted by $g \equiv [L][T]^{-2}$, and time is measured relative to a time scaling frequency, $\Omega \equiv [T]^{-1}$. Choose J_1 to be one of $\{J_1^{xx}, J_1^{yy}, \text{or } J_1^{zz}\}$. When the axis about which the inertia J_1 is computed is considered, the characteristic length is deduced from the characterizing parameters m_i and J_1 via the radius of gyration[11] $k_1 \equiv [L]$. Applying the Buckingham pi method (see Ref. 8), with m_1, J_1, and Ω as base variables, gives the pi groups

$$\Pi_{m_i} = m_i/m_1, \qquad \Pi_{J_i^{xx}} = J_i^{xx}/J_1, \qquad \Pi_{J_i^{yy}} = J_i^{yy}/J_1$$

$$\Pi_{J_i^{zz}} = J_i^{zz}/J_1, \qquad \Pi_{M_j} = M_j/m_1, \qquad \Pi_{I_j^h} = I_j^h/J_1$$

$$\Pi_G = g/k_1\Omega^2 \tag{1}$$

where $i \in \{1, n\}$ and $j \in \{1, p\}$. Note that the choice of the parameters of the first link as the base variables is arbitrary; any of the other links could be used as could some another set of base parameters if they were more convenient.

III. Equivalence Conditions: Flexible-Link Manipulators

The phrase, general flexible-link manipulator will refer to the class of manipulators with n flexible links, p actuators, and any link topology as defined in the rigid-link case. In the presentation of the flexible-link pi groups, each link will be assumed to be modeled as an Euler–Bernoulli beam, to bend in two directions, and to have high axial stiffness.

The variables characterizing the uniform ith link are length $l_i \equiv [L]$, linear mass density $\rho_i \equiv [M][L]^{-1}$, elastic modulus $E_i \equiv [M][L]^{-1}[T]^{-2}$, and the cross-sectional area moments of inertia $I_{x_i} \equiv [L]^4$ and $I_{y_i} \equiv [L]^4$. The area moments of inertia are used,

instead of the physical dimensions of the cross section, to allow the link to be described independently of the cross-sectional shape. The joint model, gravitational acceleration, and the time scaling frequency are the same as used for the rigid-link manipulator. As a point of reference, the dextrous body-fixed link coordinate frame for the ith link has its origin at the base of the link, with the z_i axis running along the undeflected link. The x_i and y_i axes are the principal axes of the cross section.

Applying the Buckingham pi theorem (see Ref. 8) with the variables ρ_1, l_1, and Ω results in the pi groups

$$\Pi_{\rho_i} = \rho_i/\rho_1, \qquad \Pi_{l_i} = l_i/l_1, \qquad \Pi_{E_i} = E_i\big/\rho_1\Omega^2$$

$$\Pi_{I_{x_i}} = I_{x_i}\big/l_1^4, \qquad \Pi_{I_{y_i}} = I_{y_i}\big/l_1^4, \qquad \Pi_{M_j} = M_j/\rho_1 l_1$$

$$\Pi_{I_j^h} = I_j^h\big/\rho_1 l_1^3, \qquad \Pi_G = g\big/l_1\Omega^2 \tag{2}$$

where $i \in \{1, n\}$ and $j \in \{1, p\}$.

Notice that the characteristic length parameter is different between the rigid-link and flexible-link manipulators, k_1 vs l_1, respectively. In a hybrid rigid-flexible link system, either parameter can be used as the representative length parameter provided that the same parameter be used consistently for all length scaling.

From the flexible link pi groups (2), the scaling condition for the natural frequencies can be determined. Consider the ith flexible-link manipulator link, and denote the natural frequency of the kth mode by $\omega_k \equiv [T]^{-1}$. Hence, ω_k can be nondimensionalized by the time scaling frequency Ω, that is,

$$\omega_k \equiv [T]^{-1} \Rightarrow \Pi_{\omega_k} \triangleq \omega_k/\Omega \tag{3}$$

The scaling law for the nondimensional frequency results naturally from the flexible link pi groups defined in Eq. (2). This can be shown using the relationship (for the ith link)[12]

$$\omega_k = \sqrt{E_i I_{x_i}\big/\rho_i l_i^4}\,\beta_k, \qquad k \in [1, \infty], \qquad i \in [1, n] \tag{4}$$

where for an Euler–Bernoulli beam model of the link, β_k is the kth solution of

$$\rho_i l_i^3\big/I_i^h\beta_k^3[\cosh(\beta_k)\sin(\beta_k) - \sinh(\beta_k)\cos(\beta_k)] + [1 + \cos(\beta_k)\cosh(\beta_k)] = 0 \tag{5}$$

as given by Bellezza et al.[13] Therefore, the frequency pi group is

$$\Pi_{\omega_k} = \omega_k/\Omega = \sqrt{\left(E_i\big/\rho_i\Omega^2\right)\left(I_{x_i}\big/l_i^4\right)}\beta_k = \sqrt{\left(\Pi_{E_i}\big/\Pi_{\rho_i}\right)\left(\Pi_{I_{x_i}}\big/\Pi_{l_i}^4\right)}\beta_k \tag{6}$$

and scaling the manipulator using the pi groups Π_{E_i}, Π_{ρ_i}, $\Pi_{I_{x_i}}$, and Π_{l_i} guarantees that the natural frequencies will scale by Ω.

Denote the transverse deflection of the ith link by $w_{x_i}(z_i, t)$. Assuming that w_{x_i} can be expressed via a modal expansion[14] results in

$$w_{x_i}(z_i, t) = \sum_{k=1}^{\infty} \phi_{x_k}(z_i)q_k(t) \tag{7}$$

Because $w_{x_i} \equiv [L]$, it can be nondimensionalized by l_1 (Ref. 8),

$$\Pi_{w_{x_i}} = \frac{w_{x_i}}{l_1} = \frac{1}{l_1}\sum_{k=1}^{\infty}\phi_{x_k}(z_i)q_k(t) \tag{8}$$

and the nondimensional group for the mode shapes is $\Pi_{\phi_{x_k}} = \phi_{x_k}/l$.

If the material density of the ith link is specified in terms of the volume mass density ρ_i^v, instead of the linear mass density ρ_i, then the flexible link pi groups that would be different from those in Eq. (2) are[8]

$$\Pi_{\rho_i} = \rho_i^v\big/\rho_1^v, \qquad \Pi_{E_i} = E_i\big/\rho_1^v l_1^2\Omega^2$$

$$\Pi_{M_j} = M_j\big/\rho_1^v l_1^3, \qquad \Pi_{I_j^h} = I_j^h\big/\rho_1^v l_1^5 \tag{9}$$

IV. Tolerances on Pi Groups

Theoretically, two systems are dynamically equivalent if and only if the values for their pi groups are exactly the same, but, because of manufacturing imprecision, it is impossible to achieve the exactness required for dynamic equivalence. The value for a nondimensional group may be close to the value required for dynamic equivalence, but will not be exactly the required value.

To allow the preceding scaling theory to be used, the sensitivity of the manipulator dynamics to changes in the nondimensional groups must be determined. If the dynamics are insensitive to the deviation of the actual pi-group values from those required for dynamic equivalence, then the two systems will be considered to be dynamically equivalent. A method will be presented that uses nonlinear feedback to render two systems that are nearly dynamically equivalent exactly dynamically equivalent.

A. Sensitivity Analysis

When two manipulators are dynamically equivalent, the nondimensional dynamics of the two manipulators are identical. If the values of the pi groups for one of the manipulators have deviated from the values required for dynamic equivalence, the nondimensional dynamics will no longer be identical, but the structure of the equations of motion will remain the same. What has to be measured, therefore, is the sensitivity of each nondimensional generalized coordinate $\hat{q}_i(\tau)$, where τ is nondimensional time, to changes in each pi group Π_j in the nondimensional dynamic equations.

The nondimensional equations describing the free motion of an unconstrained manipulator can be written as[15]

$$\hat{\boldsymbol{M}}(\hat{\boldsymbol{q}})\ddot{\hat{\boldsymbol{q}}} + \hat{\boldsymbol{C}}(\hat{\boldsymbol{q}}, \dot{\hat{\boldsymbol{q}}}) + \hat{\boldsymbol{G}}(\hat{\boldsymbol{q}}) = \hat{\boldsymbol{F}}(\tau) \tag{10}$$

where $\hat{\boldsymbol{M}}$ is the nondimensional inertia matrix, $\hat{\boldsymbol{C}}$ is the nondimensional Coriolis and centripetal acceleration vector, $\hat{\boldsymbol{G}}$ is the nondimensional gravity vector, $\hat{\boldsymbol{F}}$ is the nondimensional external generalized force vector, $\hat{\boldsymbol{q}}$ are the nondimensional generalized coordinates. Notice that $\hat{\boldsymbol{M}}$, $\hat{\boldsymbol{C}}$, and $\hat{\boldsymbol{G}}$ are functions of the pi groups, denoted by $\boldsymbol{\Pi}$. Therefore, the generalized coordinates $\hat{\boldsymbol{q}}$ are also functions of $\boldsymbol{\Pi}$. The goal of the sensitivity analysis is to find the change in each $\hat{q}_i$ caused by a change in each Π_j. The sensitivity of the joint velocities $\dot{\hat{q}}_i$ and the joint accelerations $\ddot{\hat{q}}_i$ to parameter changes also provides informative results. Throughout this section, sensitivity will be used to describe the rate of change of one quantity with respect to another. This same terminology is used by Takahashi in applying sensitivity analysis to robotic manipulators.[16]

The manipulator dynamic equation (10) can be written as a function of one of the nondimensional groups Π_j:

$$\hat{\boldsymbol{M}}[\hat{\boldsymbol{q}}(\tau; \Pi_j), \Pi_j]\ddot{\hat{\boldsymbol{q}}}(\tau; \Pi_j) + \hat{\boldsymbol{C}}[\hat{\boldsymbol{q}}(\tau; \Pi_j), \dot{\hat{\boldsymbol{q}}}(\tau; \Pi_j), \Pi_j] + \hat{\boldsymbol{G}}[\hat{\boldsymbol{q}}(\tau; \Pi_j), \Pi_j] = \hat{\boldsymbol{F}}(\tau) \tag{11}$$

Take the derivative of Eq. (11) with respect to Π_j to find

$$\hat{\boldsymbol{M}}\frac{\partial\ddot{\hat{\boldsymbol{q}}}}{\partial\Pi_j} + \left(\frac{\partial\hat{\boldsymbol{M}}}{\partial\Pi_j} + \sum_{i=1}^{n}\frac{\partial\hat{\boldsymbol{M}}}{\partial\hat{q}_i}\frac{\partial\hat{q}_i}{\partial\Pi_j}\right)\ddot{\hat{\boldsymbol{q}}} + \frac{\partial\hat{\boldsymbol{C}}}{\partial\Pi_j} + \sum_{i=1}^{n}\frac{\partial\hat{\boldsymbol{C}}}{\partial\hat{q}_i}\frac{\partial\hat{q}_i}{\partial\Pi_j} + \sum_{i=1}^{n}\frac{\partial\hat{\boldsymbol{C}}}{\partial\dot{\hat{q}}_i}\frac{\partial\dot{\hat{q}}_i}{\partial\Pi_j} + \frac{\partial\hat{\boldsymbol{G}}}{\partial\Pi_j} + \sum_{i=1}^{n}\frac{\partial\hat{\boldsymbol{G}}}{\partial\hat{q}_i}\frac{\partial\hat{q}_i}{\partial\Pi_j} = 0 \tag{12}$$

Because $\hat{\boldsymbol{M}}$ is an inertia matrix, it is always positive definite, and so from Eq. (12), the joint acceleration sensitivity can be found to be

$$\frac{\partial\ddot{\hat{\boldsymbol{q}}}}{\partial\Pi_j} = -\hat{\boldsymbol{M}}^{-1}\left[\left(\frac{\partial\hat{\boldsymbol{M}}}{\partial\Pi_j} + \sum_{i=1}^{n}\frac{\partial\hat{\boldsymbol{M}}}{\partial\hat{q}_i}\frac{\partial\hat{q}_i}{\partial\Pi_j}\right)\ddot{\hat{\boldsymbol{q}}} + \frac{\partial(\hat{\boldsymbol{C}} + \hat{\boldsymbol{G}})}{\partial\Pi_j} + \sum_{i=1}^{n}\frac{\partial(\hat{\boldsymbol{C}} + \hat{\boldsymbol{G}})}{\partial\hat{q}_i}\frac{\partial\hat{q}_i}{\partial\Pi_j} + \sum_{i=1}^{n}\frac{\partial\hat{\boldsymbol{C}}}{\partial\dot{\hat{q}}_i}\frac{\partial\dot{\hat{q}}_i}{\partial\Pi_j}\right] \tag{13}$$

From Eq. (11), an expression for $\ddot{\hat{\boldsymbol{q}}}$ can be found and used in Eq. (13) to give

$$\frac{\partial \ddot{\hat{\boldsymbol{q}}}}{\partial \Pi_j} = -\hat{\boldsymbol{M}}^{-1}\left[\left(\frac{\partial \hat{\boldsymbol{M}}}{\partial \Pi_j} + \sum_{i=1}^{n}\frac{\partial \hat{\boldsymbol{M}}}{\partial \hat{q}_i}\frac{\partial \hat{q}_i}{\partial \Pi_j}\right)\hat{\boldsymbol{M}}^{-1}(\hat{\boldsymbol{F}} - \hat{\boldsymbol{C}} - \hat{\boldsymbol{G}}) + \frac{\partial(\hat{\boldsymbol{C}} + \hat{\boldsymbol{G}})}{\partial \Pi_j} + \sum_{i=1}^{n}\frac{\partial(\hat{\boldsymbol{C}} + \hat{\boldsymbol{G}})}{\partial \hat{q}_i}\frac{\partial \hat{q}_i}{\partial \Pi_j} + \sum_{i=1}^{n}\frac{\partial \hat{\boldsymbol{C}}}{\partial \dot{\hat{q}}_i}\frac{\partial \dot{\hat{q}}_i}{\partial \Pi_j}\right] \quad (14)$$

Equation (14) is a second-order differential equation of the form

$$\frac{\mathrm{d}^2 \boldsymbol{X}_j}{\mathrm{d}\tau^2} = -\sum_{i=1}^{n}(\cdot)X_j^i - \sum_{i=1}^{n}(\cdot)\frac{\mathrm{d}X_j^i}{\mathrm{d}\tau} - (\cdot), \qquad X_j^i \triangleq \frac{\partial \hat{q}_i}{\partial \Pi_j} \quad (15)$$

A solution for $\boldsymbol{X}_j$ can be found numerically. With the sensitivity solution X_j^i, the variation in $\hat{q}_i$ caused by a variation in Π_j can be found. In particular,

$$X_j^i = \frac{\partial \hat{q}_i}{\partial \Pi_j} \Rightarrow X_j^i \approx \frac{\Delta \hat{q}_i}{\Delta \Pi_j} \quad (16)$$

For a given nominal trajectory, the sensitivity $\boldsymbol{X}_j(\tau)$ can be computed offline. Rearranging the preceding approximation gives

$$\Delta \hat{q}_i \approx X_j^i(\tau)\Delta \Pi_j \quad (17)$$

For each pi group Π_j, the preceding equation can be used to estimate how much the actual manipulator trajectory will vary from the nominal trajectory, for a given change in the value of the pi group. This information can be used before the construction of the manipulator to determine which components of the manipulator should be machined more precisely than others. A method of computing the sensitivity expressions for open-chain rigid-link manipulators was presented by Takahashi[16] and modified for the nondimensional dynamics by Ghanekar.[8]

The sensitivity analysis provides a way of measuring the effect of manufacturing errors in different components of the manipulator. The magnitude of these effects for each component can be assessed in simulation, before constructing the robot. For joint trajectories with a high sensitivity to particular pi groups, the components corresponding to those pi groups must be manufactured with high precision to ensure that the actual pi group value is very close to the value required for dynamic equivalence.

B. Error Compensation for Rigid-Link Manipulators

As already observed, it is unlikely that a perfectly scaled model can be built due to manufacturing tolerances, choice of materials, and our inability to build a predefined amount of friction into the model.

Consider a viscous friction model, in which the friction torque is given by $H = c_{vh}\dot{\theta}$, where $c_{v_h} \equiv [M][L]^2[T]^{-1}$. For a rigid-link manipulator with the fundamentally distinct parameters m_1, k_1, and Ω, the pi group for c_{vh} is

$$\Pi_{c_{v_h}} = c_v \big/ m_1 k_1^2 \Omega \quad (18)$$

Theoretically, using this scaling condition, the required friction constant for dynamic equivalence can be determined.[8] In practice, it is impossible to achieve a preset friction value, and dynamic equivalence will not be achieved. Because of this, friction effects are the ideal candidates for techniques that can compensate for errors in the pi groups, thereby making the actual system exhibit the desired dynamic behavior.

For rigid-link manipulators, a nonlinear feedback compensation scheme can be used to eliminate the error between the actual and desired dynamic behavior. Because this error compensation scheme is a special case of the feedback linearization technique, it is not generally applicable to flexible-link manipulators.[17]

With this approach it may appear that any deviation from the required pi-group values for dynamic equivalence can be tolerated. This is true theoretically, however, practically, the method is only feasible for small deviations in the pi groups because the error compensation is provided through compensation torques from the actuators. The greater the deviation of the actual pi-group values is from the required values, the greater is the magnitude of the compensation torques. Because the actuators are probably designed to operate within the torque range of the dynamically equivalent system, they may not be able to provide the large compensation torques required to correct for large deviations of the pi-group values from those required for dynamic equivalence.

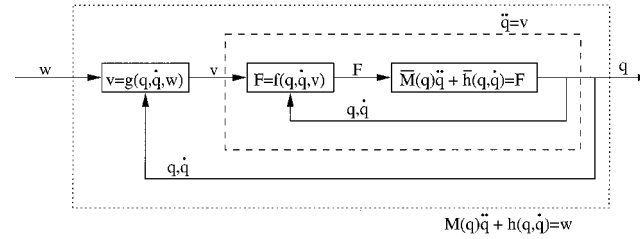

Fig. 1 Error compensation scheme using nonlinear feedback.

For the case at hand, let the desired dynamic equations be

$$\boldsymbol{M}(\boldsymbol{q})\ddot{\boldsymbol{q}} + \boldsymbol{C}(\boldsymbol{q}, \dot{\boldsymbol{q}}) = \boldsymbol{F}(t) \quad (19)$$

where $\boldsymbol{M}$, $\boldsymbol{C}$, and $\boldsymbol{F}$ are the inertia matrix; the Coriolis acceleration, centripetal acceleration, and gravity vector; and the external generalized force vector, respectively.

For this manipulator, let $\boldsymbol{\Pi}$ denote the set of pi-group values required for dynamic equivalence. Suppose, because of manufacturing imprecision, that some of the manipulator parameters are not machined to the exact specifications required for dynamic equivalence. For this manipulator, let $\bar{\boldsymbol{\Pi}}$ denote the actual values of the pi groups, where $\bar{\boldsymbol{\Pi}} \neq \boldsymbol{\Pi}$.

Let Eq. (19) denote the equations of motion of the desired (dynamically equivalent) system. For the manipulator with pi-group values $\bar{\boldsymbol{\Pi}}$, denote the "actual" equations of motion by

$$\bar{\boldsymbol{M}}(\boldsymbol{q})\ddot{\boldsymbol{q}} + \bar{\boldsymbol{C}}(\boldsymbol{q}, \dot{\boldsymbol{q}}) = \boldsymbol{F} \quad (20)$$

The objective is to use nonlinear state feedback to make the input–output dynamics between the control signal and the manipulator generalized coordinate appear as Eq. (19). In Fig. 1, the actual manipulator dynamics are represented by the block with input $\boldsymbol{F}$ and output $\boldsymbol{q}$. In addition, two nonlinear function blocks are shown in Fig. 1. Let $\boldsymbol{f}(\boldsymbol{q}, \dot{\boldsymbol{q}}, v)$ be the inner nonlinear compensation, and let $\boldsymbol{g}(\boldsymbol{q}, \dot{\boldsymbol{q}}, \boldsymbol{w})$ be the outer nonlinear compensation. The controller signal is $\boldsymbol{w}$.

The inner nonlinear block is an inverse dynamics block that makes the system from the input v to the output $\boldsymbol{q}$ appear as a double integrator.[15] The outer nonlinear block is another inverse dynamics block that makes the system from $\boldsymbol{w}$ to $\boldsymbol{q}$ exhibit the desired dynamics according to Eq. (19).

Define the inner nonlinear function $\boldsymbol{f}(\boldsymbol{q}, \dot{\boldsymbol{q}}, v)$ to be

$$\boldsymbol{F}(t) = \boldsymbol{f}(\boldsymbol{q}, \dot{\boldsymbol{q}}, v) \triangleq \bar{\boldsymbol{M}}(\boldsymbol{q})v(t) + \bar{\boldsymbol{C}}(\boldsymbol{q}, \dot{\boldsymbol{q}}) \quad (21)$$

The inertia matrix $\bar{\boldsymbol{M}}(\boldsymbol{q})$ is invertible, and hence, Eq. (20) results in the double integrator equation

$$\ddot{\boldsymbol{q}} = v(t) \quad (22)$$

Define the outer block $\boldsymbol{g}(\boldsymbol{q}, \dot{\boldsymbol{q}}, \boldsymbol{w})$ to be

$$v(t) = \boldsymbol{g}(\boldsymbol{q}, \dot{\boldsymbol{q}}, \boldsymbol{w}) \triangleq \boldsymbol{M}(\boldsymbol{q})^{-1}[-\boldsymbol{C}(\boldsymbol{q}, \dot{\boldsymbol{q}}) + \boldsymbol{w}(t)] \quad (23)$$

Substitution into Eq. (22) reveals the dynamic equation

$$\boldsymbol{M}(\boldsymbol{q})\ddot{\boldsymbol{q}} + \boldsymbol{C}(\boldsymbol{q}, \dot{\boldsymbol{q}}) = \boldsymbol{w}(t) \quad (24)$$

which represents the desired dynamics (19), with $\boldsymbol{w}$ as the input signal. This is the system from $\boldsymbol{w}$ to $\boldsymbol{q}$ in Fig. 1. The overall inverse

dynamics controller is given by combining Eqs. (21) and (23) to yield

$$\boldsymbol{F}(t) = -\bar{\boldsymbol{M}}(\boldsymbol{q})\boldsymbol{M}(\boldsymbol{q})^{-1}\boldsymbol{C}(\boldsymbol{q}, \dot{\boldsymbol{q}}) + \bar{\boldsymbol{C}}(\boldsymbol{q}, \dot{\boldsymbol{q}}) + \bar{\boldsymbol{M}}(\boldsymbol{q})\boldsymbol{M}(\boldsymbol{q})^{-1}\boldsymbol{w}(t) \quad (25)$$

The values for $\bar{\boldsymbol{M}}$ and $\bar{\boldsymbol{C}}$ are known because these represent the actual manipulator that has been constructed. The values for $\boldsymbol{M}$ and $\boldsymbol{C}$ are also known because these represent the desired dynamic behavior. Therefore, given a control input $\boldsymbol{w}(t)$, all of the quantities in Eq. (25) are known, and the control loop can be implemented. Hence, placing an inner control loop around the actual manipulator can make the manipulator exhibit the desired dynamic behavior.

The extra control effort required to achieve the desired dynamic behavior can also be calculated. Without the compensation provided by Eq. (25), $\boldsymbol{w}(t)$ is the control signal to the manipulator. Hence, the additional control effort provided by Eq. (25) can be computed by

$$\boldsymbol{F}_x(t) = \boldsymbol{F}(t) - \boldsymbol{w}(t) = -\bar{\boldsymbol{M}}(\boldsymbol{q})\boldsymbol{M}(\boldsymbol{q})^{-1}\boldsymbol{C}(\boldsymbol{q}, \dot{\boldsymbol{q}}) + \bar{\boldsymbol{C}}(\boldsymbol{q}, \dot{\boldsymbol{q}}) + (\bar{\boldsymbol{M}}(\boldsymbol{q})\boldsymbol{M}(\boldsymbol{q})^{-1} - I)\boldsymbol{w}(t) \quad (26)$$

In the limit, as the difference between the actual and desired dynamics approaches zero, the extra control effort required goes to zero.

V. Controller Scaling Laws

Let Φ define the set of m controller parameters for a general controller so that

$$\Phi \triangleq \{\phi_1, \phi_2, \ldots, \phi_m\}$$

where the fundamental dimensions of ϕ_i are assumed to be such that

$$\phi_i \equiv [M]^{a_i}[L]^{b_i}[T]^{c_i}[A]^{d_i}[\Theta]^{e_i}, \qquad a_i, b_i, c_i, d_i, e_i \in \mathbb{R}$$

To maintain the dimensional homogeneity of the system, it is imperative that for a particular manipulator system (manipulator and controller), the same base parameters are always used to compute the pi groups. Hence, select the three parameters m_1, k_1, and Ω and introduce reference values for current A_0 and temperature θ_0. The form of the scaling law for a general controller parameter ϕ_i is[8]

$$\Pi_{\phi_i} \triangleq \frac{\phi_i}{m_1^{a_i} k_1^{b_i} \Omega^{-c_i} A_0^{d_i} \theta_0^{e_i}} \quad (27)$$

For a flexible-link manipulator system, the parameter k_1 would be replaced with l_1 in the controller pi group (27).

A. Example: Sliding Mode Control

To illustrate that the methodology applies to discontinuous nonlinear controllers, this example will determine the scaling conditions for a sliding mode control law.[18] In the sliding control technique, two control inputs are designed, both of which are highly nonlinear, and the transition from one input to the other is often discontinuous.

Let the manipulator dynamics be expressed as a system of first-order differential equations

$$\dot{\boldsymbol{x}} = \boldsymbol{f}(\boldsymbol{x}) + \boldsymbol{B}\boldsymbol{u}$$

where $\boldsymbol{x}$ is the $2n \times 1$ state vector and $\boldsymbol{u}$ is the $n \times 1$ input vector.

Typically, a sliding surface is selected to be a weighted sum of joint position error and velocity error. Define the tracking error by the vector $\tilde{\boldsymbol{x}} = \boldsymbol{x} - \boldsymbol{x}_{\text{ref}}$. Then, in terms of the parameters λ_i, the sliding surfaces σ_i are defined as

$$\sigma_i(\tilde{\boldsymbol{x}}, t) = \lambda_i \tilde{x}_i + \tilde{x}_{n+i}, \qquad i \in [1, n]$$

The parameters λ_i determine the rate at which the trajectories approach the desired trajectory on the sliding surface. When

$$\boldsymbol{S} \triangleq [\text{diag}\{\lambda_1, \ldots, \lambda_n\}, I_{n \times n}]$$

is defined, then the equivalent control input is[19]

$$\hat{\boldsymbol{u}} \triangleq (\boldsymbol{SB})^{-1}(-\boldsymbol{Sf} - \boldsymbol{S}\dot{\boldsymbol{x}}_{\text{ref}})$$

The switching control input $\boldsymbol{u}^{\pm}$ drives the trajectories toward the sliding surface. In terms of the parameters K_i, this control input is defined as[19]

$$\boldsymbol{u}^{\pm} \triangleq -(\boldsymbol{SB})^{-1}[K_1 \quad \cdots \quad K_n]^T \operatorname{sgn}(\boldsymbol{\sigma}) = -(\boldsymbol{SB})^{-1}\boldsymbol{k} \operatorname{sgn}(\boldsymbol{\sigma}) \quad (28)$$

The sliding control input is given by $\boldsymbol{u} = \hat{\boldsymbol{u}} + \boldsymbol{u}^{\pm}$:

$$\boldsymbol{u}(t) \triangleq -(\boldsymbol{SB})^{-1}[\boldsymbol{Sf}(\boldsymbol{x}) + \boldsymbol{S}\dot{\boldsymbol{x}}_{\text{ref}} + \boldsymbol{k} \operatorname{sgn}(\boldsymbol{\sigma})] \quad (29)$$

A common artifact of switching controllers is a phenomenon known as chattering. The chattering effect can be smoothed out by replacing the sgn operator with a saturation operator of width Δ_i (Ref. 19) defined by

$$\operatorname{sat}\left(\frac{\sigma_i}{\Delta_i}\right) \triangleq \begin{cases} 1 & \sigma_i/\Delta_i > 1 \\ \sigma_i/\Delta_i & -1 \le \sigma_i/\Delta_i \le 1 \\ -1 & \sigma_i/\Delta_i < -1 \end{cases} \quad (30)$$

The controller parameters are

$$\Phi \triangleq \{\lambda_1, \ldots, \lambda_n, K_1, \ldots, K_n, \Delta_1, \ldots, \Delta_n\}$$

where

$$\lambda_i \equiv [T]^{-1}, \qquad K_i \equiv [T]^{-2}, \qquad \Delta_i \equiv [T]^{-1}$$

When Eq. (27) is used, the pi groups for the controller parameters are

$$\Pi_{\lambda_i} = \lambda_i/\Omega, \qquad \Pi_{K_i} = K_i/\Omega^2, \qquad \Pi_{\Delta_i} = \Delta_i/\Omega \quad (31)$$

B. Example: Proportional Derivative Control

The controller parameters are

$$\Phi \triangleq \{K_{P_1}, \ldots, K_{P_p}, K_{D_1}, \ldots, K_{D_p}\}$$

where $K_{P_j} \equiv [M][L]^2[T]^{-2}$ and $K_{D_j} \equiv [M][L]^2[T]^{-1}$. When Eq. (27) is used, the pi groups for the controller parameters are

$$\Pi_{K_{P_j}} = K_{P_j}/m_1 l_1^2 \Omega^2, \qquad \Pi_{K_{D_j}} = K_{D_j}/m_1 l_1^2 \Omega \quad (32)$$

These results are consistent with the scaling laws for linear controllers of flexible-link manipulators presented by Ghanekar et al.[1]

VI. Numerical Examples

A. Rigid-Link Manipulator and Sliding Mode Control

To illustrate the use of the dynamic equivalence conditions, a rigid two-link manipulator (Fig. 2) with rotary joints mechanically designed for use on the moon will be scaled from a lunar gravity environment to an Earth-based environment, where the development and testing will be done. The moon-based and Earth-based manipulators will be referred to as system 1 and system 2, respectively. To illustrate the controller scaling laws, a sliding mode controller

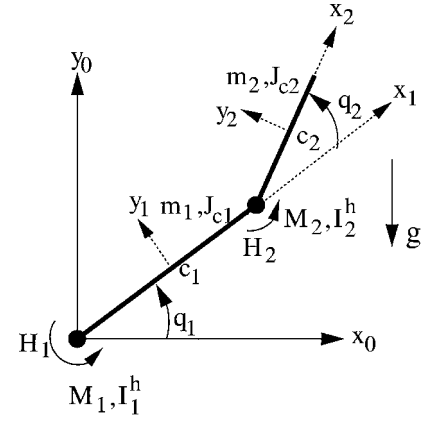

Fig. 2 Rigid two-link elbow manipulator.

designed on the prototype Earth-based manipulator will be scaled to apply to the moon-based robot.

Denote the parameters for the moon-based manipulator by the subscript m, and let the time scaling factor be $(\Omega)_m = 1\ \mathrm{s}^{-1}$. Each link is a solid cylinder with the parameters given in Table 1. Then, with $J_1 = (J_1^{xx})_m$ and $k_1 = (k_1)_m$, the pi groups [Eq. (1)] for system 1 are computed (Table 2).

In designing the Earth-based manipulator, the values for three dimensionally independent parameters can be chosen and the remaining parameters determined to satisfy the dynamic equivalence conditions (Table 2). The three chosen parameters are g_e (it cannot be altered), $m_1 = (m_1)_e$, and $J_1 = (J_1^{xx})_e$. The latter two choices are chosen simply for the purposes of the example; their choice may be driven by resource constraints imposed on the Earth-based system, for example, the system may have to be portable or may have to fit within a volume of certain dimensions. For dynamic equivalence, the remaining system parameters can be calculated from Eq. (1) and Table 2. These calculated parameters are presented in Table 3. Notice that, for system 2, the value of the time scaling parameter is $\Omega_e = 4.66\ \mathrm{s}^{-1}$. The implication of this is that the motion of the Earth-based system is approximately 4.7 times faster than the dynamically equivalent moon-based counterpart.

A sliding mode controller was designed to move system 2 from rest at the initial position of $(q_1, q_2) = (0, 0)$ to rest at the reference position: $(q_1, q_2) = (\pi/2, -\pi/2)$. The parameter values are given in Table 3. From Eq. (31), the values for the controller pi groups are calculated and are reported in Table 2. For system 1, the required sliding mode controller parameter values are presented in Table 1.

Figure 3 shows the joint angle histories for system 2 with $q_{\mathrm{ref}} = (\pi/2, -\pi/2)$. The corresponding plot for system 1 shows identical values for the joint angles, but over a time period of 23.28 s as compared to the 5 s for the Earth-based system. Figure 4 shows the torque histories for each system. The torque values for system 2 are shown on the left vertical axis and for system 1 on the right vertical axis. The Fig. 4a timescale refers to system 2 with the corresponding system 1 times given in the Fig. 4b timescale. The response of system 1 is an exact scaled version of the system 2 response and the response of the moon-based manipulator could have been predicted directly from the Earth-based prototype.

Because the Earth-based and Moon-based manipulator systems are dynamically equivalent, all of the nondimensional values for

Table 1 Parameters for moon-based manipulator (system 1)

Parameter	Variable	Value
Link length, m	$(l_{1,2})_m$	5.0
Link radius, m	$(r_{1,2})_m$	0.04
Radius of gyration, m	$(k_{1,2})_m$	0.0272
Link mass, kg	$(m_{1,2})_m$	60.0
Link inertia, $\mathrm{kg}\cdot\mathrm{m}^2$	$(J_{1,2}^{xx})_m$	0.044
Link inertia, $\mathrm{kg}\cdot\mathrm{m}^2$	$(J_{1,2}^{yy})_m$	125.02
Link inertia, $\mathrm{kg}\cdot\mathrm{m}^2$	$(J_{1,2}^{zz})_m$	125.02
Joint mass, kg	$(M_1)_m$	12.0
Joint mass, kg	$(M_2)_m$	6.0
Joint inertia, $\mathrm{kg}\cdot\mathrm{m}^2$	$(I_{1,2}^h)_m$	3.0
Gravity, $\mathrm{m}\cdot\mathrm{s}^{-2}$	$(g)_m$	1.64
Timescaling, s^{-1}	$(\Omega)_m$	1.0
s^{-1}	$\lambda_{1,2}$	1.76
s^{-2}	$K_{1,2}$	10
s^{-1}	$\Delta_{1,2}$	0.03

Table 2 Pi groups for two-link elbow manipulator

Pi group	Form	Value
Π_{m_i}	$m_{1,2}/m_1$	1.0
$\Pi_{J_i^{xx}}$	$J_{1,2}^{xx}/J_1$	1.0
$\Pi_{J_i^{yy}}$	$J_{1,2}^{yy}/J_1$	2813.0
$\Pi_{J_i^{zz}}$	$J_{1,2}^{zz}/J_1$	2813.0
Π_{M_j}	M_1/m_1	0.2
Π_{M_j}	M_2/m_1	0.1
$\Pi_{I_j^h}$	$I_{1,2}^h/J_1$	67.5
Π_G	$g/k_1\Omega^2$	60.0737
Π_{λ_i}	$\lambda_{1,2}/\Omega$	1.76
Π_{K_i}	$K_{1,2}/\Omega^2$	0.31
Π_{Δ_i}	$\Delta_{1,2}/\Omega$	0.03

Table 3 Parameters for Earth-based manipulator (system 2)

Parameter	Variable	Value
Link length, m	$(l_{1,2})_m$	1.38
Link radius, m	$(r_{1,2})_m$	0.01
Link mass, kg	$(m_{1,2})_e$	1.27
Link inertia, $\mathrm{kg}\cdot\mathrm{cm}^2$	$(J_{1,2}^{xx})_e$	0.72
Link inertia, $\mathrm{kg}\cdot\mathrm{m}^2$	$(J_{1,2}^{yy})_e$	0.20
Link inertia, $\mathrm{kg}\cdot\mathrm{m}^2$	$(J_{1,2}^{zz})_e$	0.20
Radius of gyration, m	$(k_1)_e$	0.0075
Joint mass, kg	$(M_1)_e$	0.25
Joint mass, kg	$(M_2)_e$	0.13
Joint inertia, $\mathrm{kg}\cdot\mathrm{m}^2$	$(I_{1,2}^h)_e$	0.0049
Gravity, $\mathrm{m}\cdot\mathrm{s}^{-2}$	$(g)_e$	9.81
Timescaling, s^{-1}	$(\Omega)_e$	4.66
s^{-1}	$\lambda_{1,2}$	10
s^{-2}	$K_{1,2}$	10
s^{-1}	$\Delta_{1,2}$	0.17

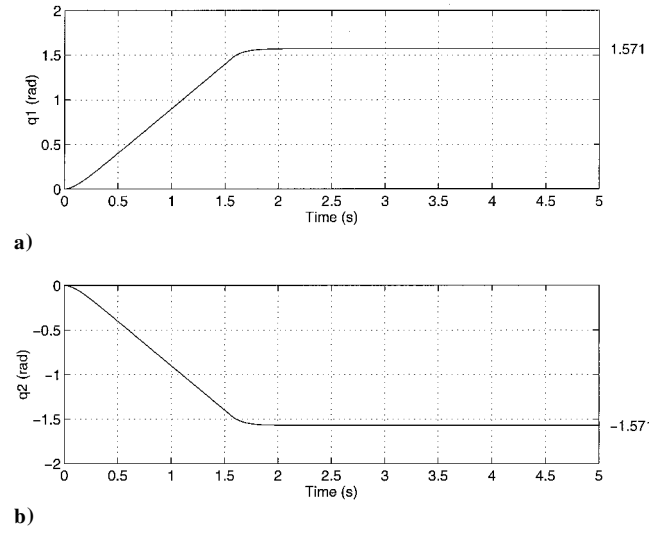

Fig. 3 Earth system: joint angles $q_{\mathrm{ref}} = (\pi/2, -\pi/2)$.

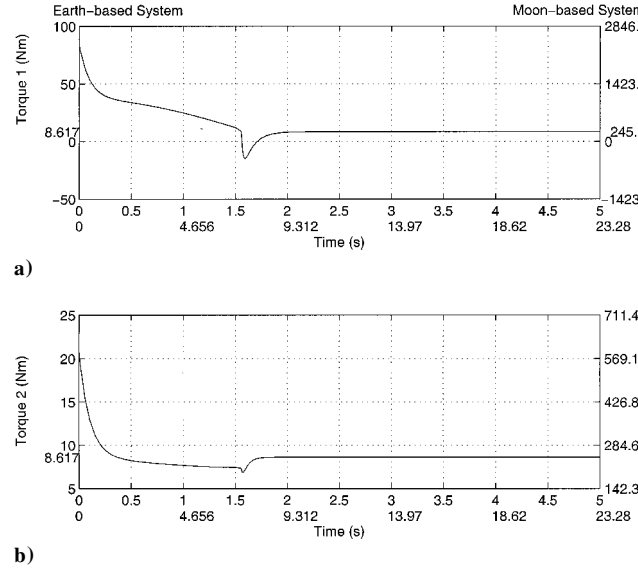

Fig. 4 Earth and moon systems: control torques $q_{\mathrm{ref}} = (\pi/2, -\pi/2)$.

both systems must be equal. Therefore, time

$$\tau = (\Omega)_m t_m = (\Omega)_e t_e \Rightarrow t_m = 4.66 t_e$$

and torque

$$\hat{H} = \frac{H_m}{\left(m_1 k_1^2 \Omega^2\right)_m} = \frac{H_e}{\left(m_1 k_1^2 \Omega^2\right)_e} \Rightarrow H_m = 28.46 H_e$$

where the actual scaling values are obtained from the system parameters for this example. Therefore, stretching the time axis of the Earth-based system responses by a factor of 4.66 will give the time axis for the moon-based system responses. Similarly, the torques are scaled by a factor of 28.46.

B. Flexible-Link Manipulator and Proportional Derivative Control

Two single flexible-link manipulators, controlled using proportional derivative (PD) control, are considered. One is intended for use on Earth and the other is intended for use on the moon. There are two rotary actuators at the base of each link to provide excitation for the horizontal and vertical vibrations; for simplicity, damping and friction effects are neglected. The equations of motion can be found in Refs. 3 and 20.

The Earth-based link is assumed to be a uniform square member with the dimensions, mass, and hub data as given in Table 4. The base parameters are $(\rho^v)_e$, $(l)_e$, and $(\Omega)_e$. Because the volume mass density $(\rho^v)_e$ is specified instead of linear mass density, the modified flexible pi groups from Eq. (9) are used (Table 5). Using Eqs. (4) and (5), with $(\beta_1)_e = 1.952$, the frequency of the first mode of vibration is $(\omega_1)_e = 55.59\ \text{s}^{-1}$.

For the moon-based manipulator, the material fixes two parameters, E_m and $(\rho^v)_m$, and the gravitational acceleration g_m fixes the third. The dimensional parameter values required for similitude are given in Table 6.

Both systems are controlled using a PD control law, and both actuators use the same controller. For the Earth-based link, the PD gains are given in Table 4, the corresponding pi groups in Table 5, and the PD gains for the moon-based link in Table 6.

Both joints were moved through a step of one radian. This was sufficient to induce both horizontal and vertical oscillations in the link. For each system, tip deflection, tip position, and control effort are given (Figs. 5–7). As expected, each pair of Figs. 5–7 are scaled versions of each other. Using subscripts e and m, to denote each system, the scaling factors for time t, lengths $\mathcal{L}$, and torques H, respectively, are

$$t_m = t_e \frac{\Omega_e}{\Omega_m} = 5.85 t_e, \qquad \mathcal{L}_m = \mathcal{L}_e \frac{(l_1)_m}{(l_1)_e} = 5.70 \mathcal{L}_e$$

$$H_m = H_e \frac{\left(m_1 l_1^2 \Omega^2\right)_m}{\left(m_1 l_1^2 \Omega^2\right)_e} = 32.51 H_e$$

In particular, the timescaling factor indicates that a motion on the moon will take almost six times longer to execute than the corresponding motion on the Earth.

Table 4 Parameters for single flexible link manipulator (Earth based)

Parameter	Variable	Value
Link length, m	l_e	1.0
Link side length, m	d_e	0.01
Link mass, kg	m_e	0.27
Link area moment of inertia, cm^4	$(I_x)_e$	0.083
	$(I_y)_e$	0.083
Young's modulus, GPa	E_e	69.0
Density, kg/m^3	ρ_e^v	2700
First natural frequency, s^{-1}	$(\omega_1)_e$	55.59
Joint inertia, $\text{kg} \cdot \text{m}^2$	$(I_j^h)_e$	0.5
Gravity, $\text{m} \cdot \text{s}^{-2}$	g_e	9.81
Timescaling, s^{-1}	Ω_e	1
Proportional gain	$(K_p)_e$	5.0
Derivative gain	$(K_d)_e$	1.0

Table 5 Pi groups for the single flexible link manipulator

Pi group	Form	Value
Π_{I_x}	$(I_x/l^4)_e$	8.3×10^{-10}
Π_{I_y}	$(I_y/l^4)_e$	8.3×10^{-10}
Π_E	$(E/\rho^v l^2 \Omega^2)_e$	2.56×10^{11}
$\Pi_{I_{1,2}^h}$	$(I_j^h/\rho^v l^3)_e$	1.85×10^{-4}
Π_G	$(g/d\Omega^2)_e$	9.81
Pi_ω	$(\omega/\Omega)_e$	55.59
Π_{Kp}	$(K_{pi}/m_i l^2 \Omega^2)_e$	18.519
Π_{Kd}	$(K_{di}/m_i l^2 \Omega)_e$	3.704

Table 6 Parameters for the single flexible link manipulator (moon based)

Parameter	Variable	Value
Link length, m	l_m	5.7
Link side length, m	d_m	0.057
Link area moment of inertia, cm^4	$(I_x)_m$	88.1
	$(I_y)_m$	88.1
Young's Modulus, GPa	E_m	12.1
Density, kg/m^3	$(\rho^v)_m$	498.2
First natural frequency, s^{-1}	$(\omega_1)_m$	9.50
Joint inertia, $\text{kg} \cdot \text{m}^2$	$(I_j^h)_m$	556.2
Gravity, $\text{m} \cdot \text{s}^{-2}$	g_m	1.635
Timescaling, s^{-1}	Ω_m	0.17
Proportional gain	$(K_p)_m$	162.57
Derivative gain	$(K_d)_m$	190.19

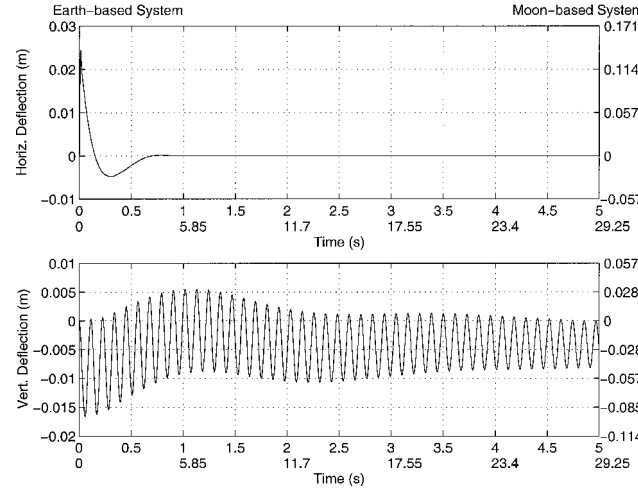

Fig. 5 Earth and moon systems: tip deflection.

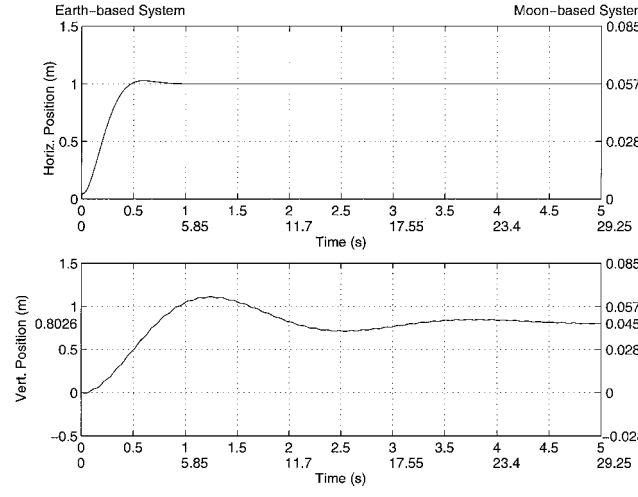

Fig. 6 Earth and moon systems: tip position.

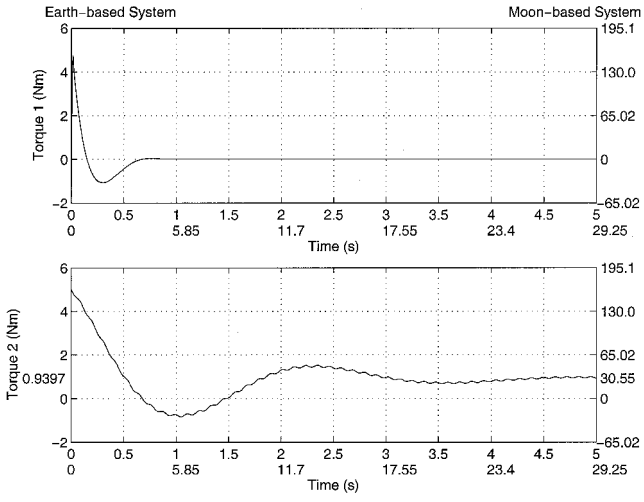

Fig. 7 Earth and moon systems: control effort.

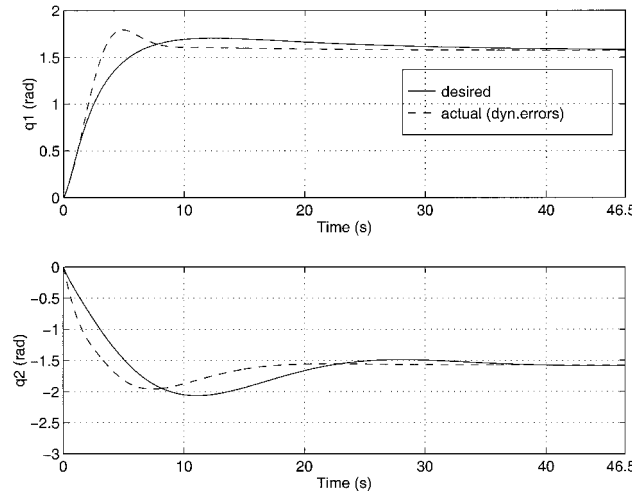

Fig. 8 Moon-based with errors: joint angles.

C. Nonlinear Compensation Technique Example

Because of manufacturing imprecision, it is impossible to construct a manipulator such that the pi-group values required for dynamic equivalence are exactly attained. In Sec. IV, it was shown that, for rigid-link manipulators, a nonlinear feedback loop can be implemented around the manipulator, such that the manipulator and nonlinear feedback together provide the required dynamic behavior.

In this example, the same Earth-based and moon-based elbow manipulators from Sec. VI.A are examined, and viscous friction is added to each joint. For the Earth-based manipulator, suppose that the friction coefficient c_v has the value $(c_v)_e = 50\ \text{kg} \cdot \text{m}^2 \cdot \text{s}^{-1}$ for both joints, and the corresponding pi group is computed [using Eq. (18)] to be $\Pi_{c_v} = 1.49 \times 10^5$.

Parameter values for the moon-based manipulator that are required for dynamic equivalence were computed in the earlier example. In addition, the friction coefficient required for dynamic equivalence can be found using Π_{c_v} to be $(c_v)_m = (m_1)_m (k_1)_m^2 (\Omega)_m \Pi_{c_v} = 6630\ \text{kg} \cdot \text{m}^2 \cdot \text{s}^{-1}$. Notice that the magnitude of the friction coefficient has changed by a significant factor (from 50 to $6630\ \text{kg} \cdot \text{m}^2 \cdot \text{s}^{-1}$).

Suppose a dynamically equivalent Earth-based manipulator was designed and built to provide the desired performance. Now, a moon-based manipulator must be designed so it can replicate this performance, but suppose that, after it has been assembled, it is found that there is an error between the actual and desired values for some of the the manipulator parameters. Because of this, the pi-group values are not equal to those required for dynamic equivalence, and hence, the Moon based manipulator is dynamically "inequivalent" to the Earth-based prototype. For this example, the following arbitrary errors were introduced: m_2, 50% error; J_1^{yy} and J_2^{yy}, 100% error; M_1, 50% error; I_2^h, 75% error; and c_v, 4900% error. The errors were purposefully made large to be able to illustrate the effect of having pi-group values other than those required for dynamic equivalence. The error for the friction coefficient is the largest because the friction coefficient was not changed to the required value ($6630\ \text{kg} \cdot \text{m}^2 \cdot \text{s}^{-1}$), but was kept at $c_v = 50\ \text{kg} \cdot \text{m}^2 \cdot \text{s}^{-1}$ for both systems.

When the scaled proportional integral derivative (PID) controller is used, the manipulator is moved from $(q_1, q_2) = (0, 0)$ to $(\pi/2, -\pi/2)$. The joint angle response is given in Fig. 8. It is clear that the response is not that desired for dynamic equivalence (dashed line).

To remedy the situation, the error compensation technique of Sec. IV.B is implemented. From the values for the pi groups, the parameter values for the dynamically equivalent moon manipulator are known and allow calculation of the desired inertia matrix $\boldsymbol{M}$ and the Coriolis acceleration, centripetal acceleration, and gravity effects vector $\boldsymbol{C}$. With the errant values for the parameters specified earlier, the actual inertia matrix $\tilde{\boldsymbol{M}}$ and the actual Coriolis, centripetal, and gravity effects vector $\tilde{\boldsymbol{C}}$ are also calculated. With these matrices and the PID controller signal, the error compensation torque from Eq. (25) is implemented.

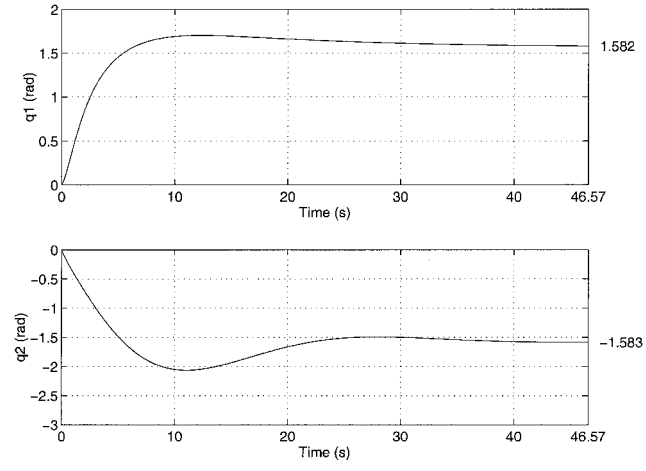

Fig. 9 Moon-based with compensation: joint angles.

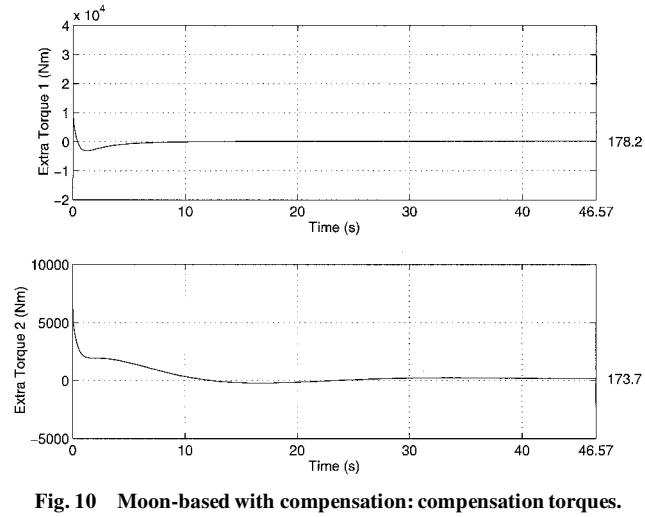

Fig. 10 Moon-based with compensation: compensation torques.

The same motion is now performed with the scaled PID controller and the error compensation. The desired scaled performance is achieved (Fig. 9), but at the expense of extra compensation torque provided by the inner compensation loop, as shown in Fig. 10.

VII. Summary

Dynamic equivalence conditions for general rigid-link and general flexible-link manipulators were derived, and the scaling laws for general nonlinear controllers were also presented. For flexible-link manipulators, scaling conditions were found for the natural

frequencies, mode shapes, damping effects, and torsional effects. To tolerate errors in the scaling conditions, a compensation technique using a double inverse dynamics loop was presented. The manipulator and controller scaling conditions were illustrated via simulation examples. The rigid-link manipulator/sliding-mode example and the flexible-link manipulator/PD control example both showed that two physically different, yet dynamically equivalent, manipulators can be constructed that produce scaled responses with the application of scaled controllers. In particular, the flexible-link example showed that the natural frequencies do indeed scale between dynamically equivalent systems. The error compensation scheme example illustrated how the proposed double inverse-dynamics loop can be used to compensate for errors in the scaling conditions caused by friction.

References

[1]Ghanekar, M., Wang, D. W. L., and Heppler, G. R., "Scaling Laws for Linear Controllers of Flexible Link Manipulators Characterized by Nondimensional Groups," *IEEE Transactions on Robotics and Automation*, Vol. 13, No. 1, 1997, pp. 117–127.

[2]Hollerbach, J. M., "Dynamic Scaling of Manipulator Trajectories," *Journal of Dynamic Systems, Measurement and Control*, Vol. 106, No. 1, 1984, pp. 102–106.

[3]Youcef-Toumi, K., and Gutz, D. A., "Impact and Force Control: Modelling and Experiments," *Journal of Dynamic Systems, Measurement and Control*, Vol. 116, No. 1, 1994, pp. 89–98.

[4]Goldfarb, M., "Dimensional Analysis and Selective Distortion in Scaled Bilateral Telemanipulation," *Proceedings of the 1998 IEEE International Conference on Robotics and Automation*, Vol. 2, 1998, Inst. of Electrical and Electronics Engineers, New York, pp. 1609–1614.

[5]Stocco, L., Salcudean, S. E., and Sassani, F., "Matrix Normalization for Optimal Robot Design," *Proceedings of the 1998 IEEE International Conference on Robotics and Automation*, Vol. 2, 1998, Inst. of Electrical and Electronics Engineers, New York, pp. 1346–1351.

[6]Ghanekar, M., Wang, D. W. L., and Heppler, G. R., "Scaling Laws for Nonlinear Controllers of Dynamically Equivalent Rigid-Link Manipulators," *Proceedings of the 1998 IEEE International Conference on Robotics and Automation*, Vol. 3, 1998, Inst. of Electrical and Electronics Engineers, New York, pp. 2633–2639.

[7]Ghanekar, M., Wang, D. W. L., and Heppler, G. R., "Scaling Laws for the Dynamics and Control of Flexible-Link Manipulators," *Proceedings of the 1999 IEEE International Conference on Robotics and Automation*, 1999, Inst. of Electrical and Electronics Engineers, New York, pp. 427–434.

[8]Ghanekar, M., "Dynamic Equivalence Conditions and Controller Scaling Laws for Robotic Manipulators," Ph.D. Dissertation, Dept. of Electrical and Computer Engineering, Univ. of Waterloo, Waterloo, ON, Canada, 1997.

[9]*Canadian Metric Practice Guide (CAN3-Z234.1-89).* Canadian Standards Association, Rexdale, ON, Canada, 1989, p. 9.

[10]Bridgman, P. W., *Dimensional Analysis*, Yale Univ. Press, New Haven, CT, 1931, pp. 36–46.

[11]Greenwood D. T., *Principles of Dynamics*, Prentice–Hall, Upper Saddle River, NJ, 1988, p. 304.

[12]Meirovitch, L., *Analytical Methods in Vibrations*, MacMillan, Toronto, 1969.

[13]Bellezza, F., Lanari, L., and Ulivi, G., "Exact Modelling of the Flexible Slewing Link," *Proceedings of the 1990 IEEE International Conference on Robotics and Automation*, Vol. 3, 1990, Inst. of Electrical and Electronics Engineers, New York, pp. 734–739.

[14]Humar, J. L., *Dynamics of Structures*, Prentice–Hall, Englewood Cliffs, Upper Saddle River, NJ, 1990, pp. 663–668.

[15]Spong, M. W., and Vidyasagar, M., *Robot Dynamics and Control*, Wiley, New York, 1989, pp. 141–143.

[16]Takahashi, T., "A Method of Sensitivity Analysis and its Applications to Robot Manipulators," *Control-Theory and Advanced Technology*, Vol. 3, No. 1, 1987, pp. 73–84.

[17]Wang, D., and Vidyasagar, M., "Control of a Class of Manipulators with the Last Link Flexible—Part I, Feedback Linearization," *Journal of Dynamic Systems, Measurement and Control*, Vol. 113, No. 4, 1991, pp. 655–661.

[18]DeCarlo, R. H., Zak, S. H., and Matthews, G. P., "Variable Structure Control of Nonlinear Multivariable Systems," *Proceedings of the IEEE*, Vol. 76, No. 3, 1988, pp. 212–232.

[19]Slotine, J., and Li, W., *Applied Nonlinear Control*, Prentice–Hall, Upper Saddle River, NJ, 1991, pp. 276–307.

[20]Ding, X., Tarn, T., and Bejczy, A. K., "A Novel Approach to the Modelling and Control of Flexible Robot Arms," *Proceedings of the 27th IEEE Conference on Decision and Control*, Vol. 1, Inst. of Electrical and Electronics Engineers, New York, 1988, pp. 52–57.

E. R. Johnson
Associate Editor